


Higher-order topological degeneracies and progress towards unique successive state switching in a four-level open system

Sayan Bhattacharjee ¹, Harsh K. Gandhi ¹, Arnab Laha ^{1,2} and Somnath Ghosh ^{1,*}

¹*Unconventional Photonics Laboratory, Department of Physics, Indian Institute of Technology Jodhpur, Rajasthan 342037, India*

²*Institute of Radiophysics and Electronics, University of Calcutta, Kolkata 700009, India*



(Received 12 August 2019; published 23 December 2019)

The physics of topological singularities, namely, exceptional points (EPs), has been a key to a wide range of intriguing and unique physical effects in non-Hermitian systems. In this context, exploration of the mutual interactions among the states in four-level systems around fourth-order EPs (EP4s) is lacking. Here we report a four-level parameter-dependent perturbed non-Hermitian Hamiltonian, mimicking quantum or wave-based systems, to explore the physical aspects of an EP4 analytically as well as numerically. The proposed Hamiltonian exhibits different orders of interaction schemes with the simultaneous presence of different higher-order EPs. Here an EP4 has been realized by mutual interaction between four states with proper parameter manipulation. We comprehensively investigate the dynamics of corresponding coupled eigenvalues with stroboscopic parametric variation in the vicinity of the embedded EP4 to establish a successive state-switching phenomenon among them, which proves to be robust even in the presence of different orders of EPs. Implementing the relation of the perturbation parameters with the coupling control parameters, we report a region to host multiple EP4s in a specific system. The chiral behavior of successive state exchange has also been established near the EP4. The proposed scheme, which is enriched with physical aspects of EP4s, should provide a unique light manipulation tool in any anisotropic multistate integrated system.

DOI: [10.1103/PhysRevA.100.062124](https://doi.org/10.1103/PhysRevA.100.062124)

I. INTRODUCTION

Beyond ideal Hermitian quantum systems, nonconservative open systems experience rich physical impacts as they interact with their surroundings and hence are either dissipative or active in nature. The non-Hermitian formulation in quantum mechanics provides useful tools to express any such open system in a matrix form which hosts discrete energy states having complex eigenvalues [1]. During the interaction between the complex states of a parameter-dependent open system, spectral degeneracies can be realized with the presence of branch-point singularities in the parameter space. An exceptional point (EP) of order N (EP N) is a special kind of topological singularity in the system parameter space of non-Hermitian systems in general, for which N number of eigenvalues and their corresponding eigenvectors simultaneously coalesce and the effective Hamiltonian of the underlying system becomes defective [2,3]. Thus, a second-order EP (EP2) refers to a particular singularity where two interacting eigenvalues coalesce [4,5]. In a very similar way, a third-order EP (EP3) can be realized with the coalescence of three interacting states [6–8]; however, there are several reports on EP3s where similar physical consequences can be achieved by winding around two EP2s associated with three interacting states [9–11]. Recently, arbitrarily higher-order EPs [12] have also been studied using various anisotropic systems [13].

In the presence of EPs, exotic physical phenomena have been widely investigated in a wide range of open systems such as atomic [14,15] and molecular [16] spectra, microwave cavities [17], Bose-Einstein systems [18], and Bose-Hubbard systems [19]. Apart from these nonoptical systems, the unconventional physical aspects of EPs have been mainly studied in various photonic systems such as lasers [20,21], optical microcavities [22–24], planar [25,26] and coupled [27–29] waveguides, and photonic crystals [30,31]. Using optical gain and loss as nonconservative elements, such photonic systems provide a leading platform to meet a wide range of contemporary technological applications such as unidirectional light transmission [32], topological energy transfer [33], asymmetric mode switching and conversion [25–28], resonance scattering [34], cross-polarization mode coupling [31,35], lasing and antilasing [20,21], ultrasensitive optical sensing [36–39], optical isolation with enhanced nonreciprocal effect [40,41], and the stopping of light [42]. Recently, EPs have been also explored in cavity optomechanics [43] in the context of phonon-magnon coupling [44] and phonon lasing [45]. In various parity-time (\mathcal{PT})-symmetric systems, EPs have been studied in connection with broken \mathcal{PT} symmetry [46]. For a detailed review, see Ref. [47].

The presence of an EP in parameter space unexpectedly modifies the dynamics of the system. A stroboscopic variation of control parameters enclosing an EP results in the permutation between the coupled states where they successively exchange their identities [5,10,11,14,15,22–26,29]. This state-exchange phenomenon around a branch-point singularity is the fundamental proof of the exceptional behavior of that

*somiit@rediffmail.com

singularity in the sense that the singularity must behave like an EP. Such an effect of parametric encirclement around an EP2 and the corresponding topological properties [48] were experimentally demonstrated for the first time in an microwave cavity [49]. During permutation between two interacting states, one of the corresponding eigenvectors acquires an additional Berry phase [50]. The successive state flipping between three coupled states around an EP3 and their corresponding geometric phase behavior have been analytically established [10,11,50] and also demonstrated numerically in a coupled waveguide system [29]. Instead of such stroboscopic parametric encirclement around EPs, for device-level implementation, if we consider time- or analogous length-scale-dependent parametric variation to encircle an EP dynamically, then the adiabaticity of the system breaks down, which essentially enables a nonadiabatic evolution of one of the two coupled states [51]. In that case, only the eigenstate that evolves with a lower average loss behaves adiabatically, and depending on the direction of rotation, a specific eigenstate dominates at the end of encirclement process. Such a competition between the effect of an EP and the adiabatic theorem leads to an asymmetric state-transfer phenomenon [25–28].

The cube-root response near an EP3 entails more complex physics in comparison with the square-root response near an EP2. For example, if we consider an EP-aided sensing application, then sensitivity can be immensely enhanced, exploiting an EP3 [38] in comparison with an EP2 [36,37]. So it would be indeed quite interesting if one can manipulate the mutual interaction between four states simultaneously, then an EP4 can be encountered which could be suitable to study the even more complex physics of the fourth-root response near the EP4. At an EP4, four interacting states should be analytically connected. However, with proper parameter manipulation, the simultaneous interaction among four states and successive exchange between them around an EP4 have never been explored.

In this paper we explore the analytical framework and corresponding topological properties of an EP4. To study the state dynamics alongside an EP4, we realize an open system, having four decaying eigenstates, that is subjected to a parameter-dependent perturbation. We judiciously choose some control parameters to connect the passive system to the perturbation in such a way that we can simultaneously study different orders of interaction phenomena. With proper parameter manipulation, we encounter a situation where four states are mutually interacting around a fourth-order singularity. Encircling this singularity in the system parameter plane, we explore an exclusive state-flipping phenomenon. Here four coupled states exchange their identities successively, which confirms the presence of an EP4. In addition to an EP4, we also explore the simultaneous existence of EP2s and EP3s in the same system and establish the possibility of the simultaneous existence of different orders of EPs in a particular system. Similar to one-dimensional exceptional-line which connect multiple EP2s [22,23], we corroborate the relation of the perturbation parameters to the coupling control parameters and formulate a three-dimensional (3D) EP4 region within which multiple locations that could be labeled as EP4s coexist. The chiral behavior of state exchange around the EP4 has also been established. The proposed scheme may be implemented using

suitable state-of-the-art techniques in an anisotropic multistate optical system.

II. MATHEMATICAL MODELING

In order to achieve our goal, we consider a simple generic 4×4 non-Hermitian Hamiltonian matrix \mathcal{H} having the form $H_0 + \lambda H_p$,

$$\mathcal{H} = \begin{pmatrix} \tilde{\epsilon}_1 & 0 & 0 & 0 \\ 0 & \tilde{\epsilon}_2 & 0 & 0 \\ 0 & 0 & \tilde{\epsilon}_3 & 0 \\ 0 & 0 & 0 & \tilde{\epsilon}_4 \end{pmatrix} + \lambda \begin{pmatrix} 0 & \omega_p & 0 & \omega_q \\ \omega_p & 0 & \omega_r & 0 \\ 0 & \omega_r & 0 & \omega_s \\ \omega_q & 0 & \omega_s & 0 \end{pmatrix}. \quad (1)$$

Here the passive Hamiltonian H_0 is subjected to a parameter-dependent complex perturbation H_p . In addition, λ represents a complex tunable parameter as $\lambda = \lambda_R + i\lambda_I$. The H_0 consists of four complex states $\tilde{\epsilon}_j$ ($j = 1, 2, 3, 4$). Here we consider $\tilde{\epsilon}_j = \epsilon_j + i\tau_j$ ($\tau_j \ll \epsilon_j$) given that τ_j are the decay rates of the respective ϵ_j . The H_p is parametrized by four interconnected perturbation parameters $\omega_p, \omega_q, \omega_r$, and ω_s . Now four eigenvalues of \mathcal{H} , say, E_j ($j = 1, 2, 3, 4$), are obtained by solving the eigenvalue equation $|\mathcal{H} - EI| = 0$ (with I the 4×4 identity matrix), which gives the quartic secular equation

$$E^4 + p_1 E^3 + p_2 E^2 + p_3 E + p_4 = 0, \quad (2)$$

where

$$p_1 = -(\tilde{\epsilon}_1 + \tilde{\epsilon}_2 + \tilde{\epsilon}_3 + \tilde{\epsilon}_4), \quad (3a)$$

$$p_2 = \tilde{\epsilon}_1 \tilde{\epsilon}_2 + \tilde{\epsilon}_2 \tilde{\epsilon}_3 + \tilde{\epsilon}_3 \tilde{\epsilon}_4 + \tilde{\epsilon}_4 \tilde{\epsilon}_1 + \tilde{\epsilon}_1 \tilde{\epsilon}_3 + \tilde{\epsilon}_2 \tilde{\epsilon}_4 - \lambda^2 (\omega_p^2 + \omega_q^2 + \omega_r^2 + \omega_s^2), \quad (3b)$$

$$p_3 = -(\tilde{\epsilon}_1 \tilde{\epsilon}_2 \tilde{\epsilon}_3 + \tilde{\epsilon}_2 \tilde{\epsilon}_3 \tilde{\epsilon}_4 + \tilde{\epsilon}_1 \tilde{\epsilon}_3 \tilde{\epsilon}_4 + \tilde{\epsilon}_1 \tilde{\epsilon}_2 \tilde{\epsilon}_4) + \lambda^2 \{ (\tilde{\epsilon}_1 + \tilde{\epsilon}_2) \omega_s^2 + (\tilde{\epsilon}_2 + \tilde{\epsilon}_3) \omega_q^2 + (\tilde{\epsilon}_3 + \tilde{\epsilon}_4) \omega_p^2 + (\tilde{\epsilon}_4 + \tilde{\epsilon}_1) \omega_r^2 \}, \quad (3c)$$

$$p_4 = \tilde{\epsilon}_1 \tilde{\epsilon}_2 \tilde{\epsilon}_3 \tilde{\epsilon}_4 - \lambda^2 (\tilde{\epsilon}_1 \tilde{\epsilon}_2 \omega_s^2 + \tilde{\epsilon}_2 \tilde{\epsilon}_3 \omega_q^2 + \tilde{\epsilon}_3 \tilde{\epsilon}_4 \omega_p^2 + \tilde{\epsilon}_4 \tilde{\epsilon}_1 \omega_r^2) - \lambda^4 (\omega_p \omega_s + \omega_q \omega_r)^2. \quad (3d)$$

Using Ferrari's method [52], the roots of Eq. (2) can be written as

$$E_{1,2} = -\frac{p_1}{4} - \eta \pm \frac{1}{2} \sqrt{-4\eta^2 - 2m_1 + \frac{m_2}{\eta}}, \quad (4a)$$

$$E_{3,4} = -\frac{p_1}{4} + \eta \pm \frac{1}{2} \sqrt{-4\eta^2 - 2m_1 - \frac{m_2}{\eta}}, \quad (4b)$$

where

$$\eta = \frac{1}{2} \sqrt{-\frac{2}{3} m_1 + \frac{1}{3} \left(\kappa + \frac{m_3}{\kappa} \right)} \quad (5)$$

$$\text{with } \kappa = \left(\frac{m_4 + \sqrt{m_4^2 - 4m_3^3}}{2} \right)^{1/3}.$$

Here

$$m_1 = -\frac{3p_1^2}{8} + p_2, \quad (6a)$$

$$m_2 = \frac{p_1^3}{8} - \frac{p_1 p_2}{2} + p_4, \quad (6b)$$

$$m_3 = p_2^2 - 3(p_1 p_3 + 4p_4), \quad (6c)$$

$$m_4 = 2p_2^3 - 9p_2(p_1 p_3 + 8p_4) + 27(p_1^2 p_4 + p_3^2). \quad (6d)$$

Thus, the roots of Eq. (2) given by Eqs. (4a) and (4b) represent the eigenvalues of \mathcal{H} . In addition, with the complex λ , we deliberately introduce a controlling parameter δ to interconnect the four perturbation parameters of H_p . Here we customize the perturbation parameters in terms of δ as

$$\omega_p = 4\delta - 10^{-4}, \quad \omega_q = \delta - 0.1, \quad (7a)$$

$$\omega_r = 0.95 - \delta/2, \quad \omega_s = 0.5 - \delta. \quad (7b)$$

The independent tunability parameter δ enables the simultaneous modulation of four perturbation parameters ω_k ($k = p, q, r, s$). Thus, with the simultaneous variation of complex λ ($=\lambda_R + i\lambda_I$) and δ , the perturbation parameters ω_k ($k = p, q, r, s$) control the interactions between the E_j ($j = 1, 2, 3, 4$). Using this framework, various interaction phenomena are described in the following section. During optimization, we choose the passive eigenvalues $\varepsilon_1 = 0.9$, $\varepsilon_2 = 0.8$, $\varepsilon_3 = 1.25$, and $\varepsilon_4 = 0.25$ with the corresponding decay rates $\tau_1 = 5 \times 10^{-3}$, $\tau_2 = 2.5 \times 10^{-3}$, $\tau_3 = 0.2 \times 10^{-3}$, and $\tau_4 = 0.01 \times 10^{-3}$. Here we consider $\tau_j \ll \varepsilon_j$ to implement this analytical model on any feasible anisotropic prototypal device.

To design a prototype by implementing the proposed scheme, one can consider a gain-loss-assisted coupled waveguide system supporting four or more channels or cores. The idea may be conceived in such a way that the physical separation between the cores and/or dimensions of individual cores may vary along the length of the device. Therefore, this four-core guided wave system would be represented by the passive Hamiltonian H_0 . Introduced gain or loss and the separation between the cores with variable dimensions along the propagation direction can be considered as a perturbation (λH_p). Here the imaginary part of complex λ , i.e., λ_I , may be deemed to be introduced gain or loss and δ may be mapped to the varying dimension of the cores or the varying separation between them. Thus, based on the proposed scheme, we enable the system to host EPs due to an anisotropic perturbation that would follow the proposed Hamiltonian. A similar gain-loss-assisted three-waveguide non-Hermitian system hosting two EP2s has been reported [28]. Here both EP2s have been encountered by varying the gain and loss, the dimension of the channels, and also the spacing between them along the length of the waveguide. Our proposed scheme can be straightforwardly implemented in an extended version of similar guided wave geometry supporting four or more channels or cores.

III. DIFFERENT ORDERS OF INTERACTIONS BETWEEN COUPLED STATES

With consideration of the specific optimized values as described in the previous section, we study the interactions between E_j ($j = 1, 2, 3, 4$), to which we simultaneously vary the complex λ and δ within judiciously chosen regions. Here λ_R varies within the range from 0.56 to 0.57, whereas λ_I varies simultaneously, maintaining the ratio $\lambda_I/\lambda_R = -10^{-3}$. The choice of λ_I of the order 10^{-3} of λ_R makes the physical system more realistic. In any prototypal guided wave geometries used to implement the proposed scheme, the cited ratio λ_I/λ_R is closer to the real attenuation or gain coefficient. The span for the variation of δ is chosen to be within $[-0.04, 0.04]$.

We study the interactions between the E_j ($j = 1, 2, 3, 4$) in Fig. 1 with an increasing λ and δ within the chosen limits. The trajectories of E_j ($j = 1, 2, 3, 4$) have been shown using dashed red, solid green, dotted blue, and solid black lines, respectively. In Fig. 1(a) we can observe the interaction between E_1 and E_2 in a certain range of control parameters (within the specified span), where E_3 and E_4 remain unaffected. The equivalent dynamics of E_j ($j = 1, 2, 3, 4$) with respect to λ_R , λ_I , and δ are depicted in Figs. 1(a i), (a ii), and (a iii), respectively. Thus, from the interaction phenomenon shown in Fig. 1, it can be inferred that there should be a singularity of second order near the interaction regime of E_1 and E_2 . Now, with a further increase in λ and δ , we observe the simultaneous interaction between E_1 , E_2 , and E_3 , not affecting E_4 , which is shown in Fig. 1(b). Here the similar behavior of E_j ($j = 1, 2, 3, 4$) concerning λ_R , λ_I , and δ , as can be seen in Figs. 1(b i), (b ii), and (b iii), respectively, supports the presence of a third-order singularity in the (λ, δ) plane. After investigating the second- and third-order interactions, we further increase the values of the control parameters to study the fourth-order interaction, which is shown in Fig. 1(c). Here we observe that for comparably higher values of λ and δ , all four states E_j ($j = 1, 2, 3, 4$) are mutually interacting and show similar coupling natures with respect to λ_R , λ_I , and δ , as depicted in Figs. 1(c i), (c ii), and (c iii), respectively. Such mutual coupling between four interacting states confirms the presence of a singularity of fourth order in the system parameter plane.

All kinds of interaction phenomena of different orders (as shown in Fig. 1), which are hosted by the Hamiltonian \mathcal{H} [given by Eq. (1)], are simultaneously presented in Fig. 2 for the entire chosen span of λ and δ . In Figs. 2(a), 2(b), and 2(c), all the interaction phenomena among the E_j are shown with respect to λ_R , λ_I , and δ , respectively, where we observe that, at the initial points of the chosen scale of the control parameters, the eigenvalues remain noninteracting, and then with an increase in parametric values, they exhibit different orders of interactions for different parametric regions. Thus identifying these particular regions in the parameter plane, we can realize the presence of singularities of different orders. In the following section we examine the exceptional behavior of the embedded singularities by moving around them in the system parameter plane.

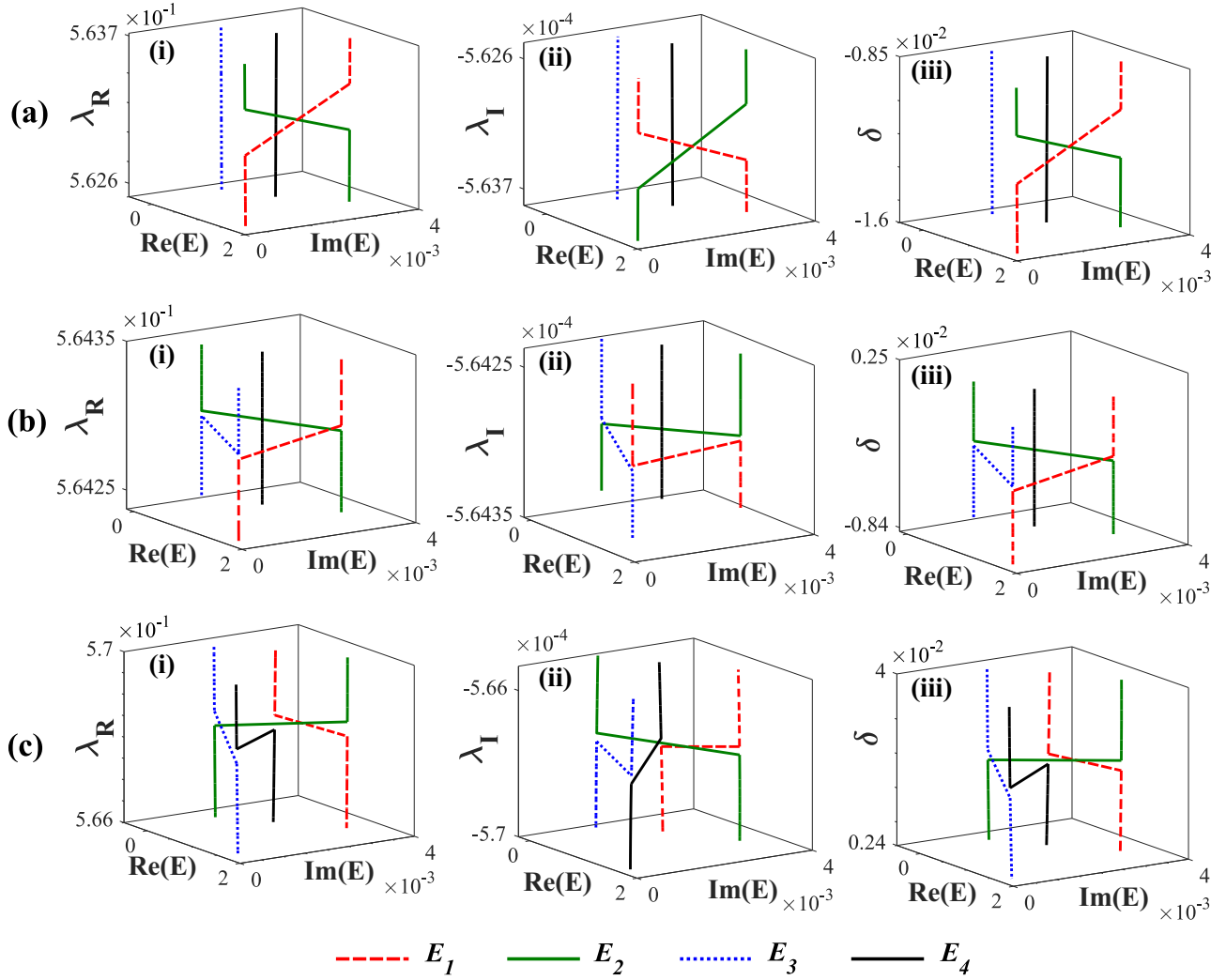


FIG. 1. Interactions between the eigenvalues with the variations of the perturbation parameters. Trajectories of E_j ($j = 1, 2, 3, 4$) are shown by dashed red, solid green (light gray), dotted blue, and solid black lines, respectively. (a) Second-order interaction between E_1 and E_2 , not affecting E_3 and E_4 , with respect to (a i) λ_R , (a ii) λ_I , and (a iii) δ . (b) Third-order interaction between E_1 , E_2 , and E_3 , not affecting E_4 , with respect to (b i) λ_R , (b ii) λ_I , and (b iii) δ . (c) Fourth-order interaction between E_1 , E_2 , E_3 , and E_4 with respect to (c i) λ_R , (c ii) λ_I , and (c iii) δ .

IV. PHYSICAL EFFECTS OF TOPOLOGICAL SINGULARITIES: TOWARDS SUCCESSIVE STATE SWITCHING

If a singularity behaves like an EP, then its presence inside the closed parameter space of the underlying system leads to significant modifications in the dynamics of the corresponding coupled states due to the influence of the coupling parameters. Quasistatically encircling an EP in parameter space results in the permutation between the coupled eigenvalues. Around an EP, the corresponding coupled eigenvalues exchange their identities adiabatically. To enclose the singularities, we use the following parametric equation in the (λ, δ) plane:

$$\lambda_R(\phi) = a_0[1 + r_1 \cos(\phi)], \quad (8a)$$

$$\delta(\phi) = b_0[1 + r_2 \sin(\phi)]. \quad (8b)$$

Here (a_0, b_0) represents the center of the parametric loop and r_1 and r_2 are two characteristic parameters to control the variations of λ_R and δ over a tunable angle ϕ given that $\phi \in [0, 2\pi]$. To encircle a singularity, we choose the variation

of λ_R and δ using Eq. (8), where there is a variation of λ_I maintaining the ratio $\lambda_I/\lambda_R = -10^{-3}$ (as mentioned in Sec. III). Such overall parameter space $(\lambda_R, \lambda_I, \delta)$ variation significantly affects the dynamics of the coupled states. Judiciously choosing the characteristics parameters of Eq. (8), we can encircle the single or multiple singularities (even the singularities having different orders) to scan the enclosed area. Now if we establish the successive state switching by parametric encirclement around the embedded singularities of different orders, then we can confirm that the proposed Hamiltonian \mathcal{H} hosts different order of EPs [5,10,11,14,15,22–26,29].

Now we predict the approximate second-order interaction region between E_1 and E_2 (except E_3 and E_4), as shown in Fig. 1(a), and judiciously choose $a_0 = 0.55$, $b_0 = -0.0178$, $r_1 = 0.05$, and $r_2 = 0.45$ to enclose the associated second-order singularity. The corresponding parametric loop is shown in Fig. 3(a). Looking at the ranges of the x and y axes of Fig. 3(a) and y axes of Figs. 1(a i) and 1(a iii), we can confirm that the described parametric loop in Fig. 3(a) perfectly encloses the associated singularity that is

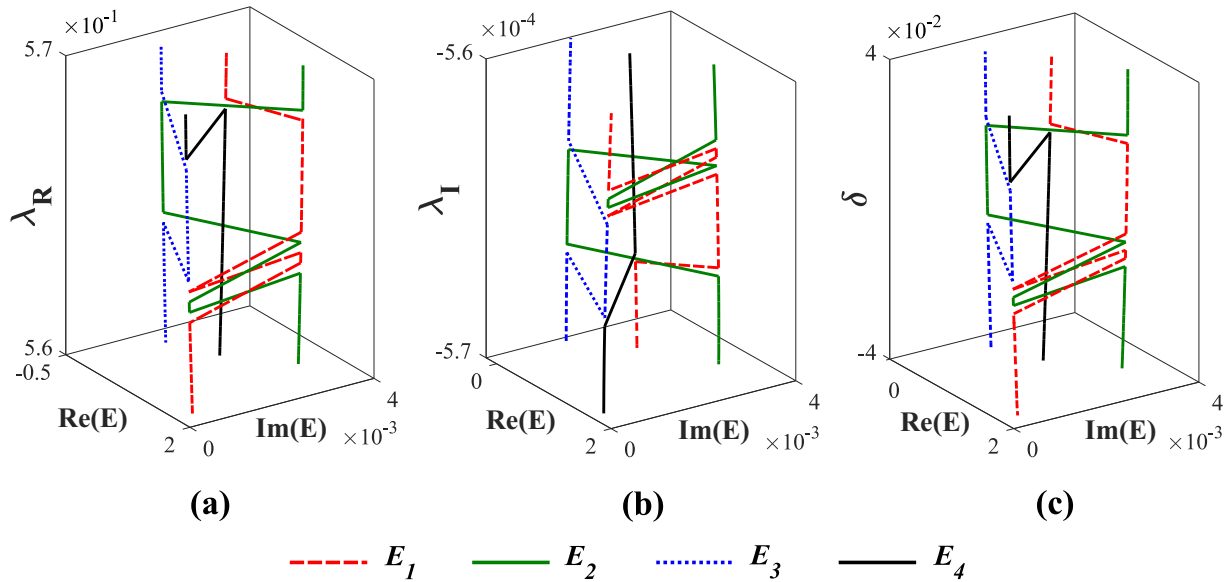


FIG. 2. Simultaneous representation of different orders of interactions shown in Fig. 1 with respect to (a) λ_R , (b) λ_I , and (c) δ within the chosen ranges.

responsible for the coupling between E_1 and E_2 . Following a very slow evolution along this parametric loop, we plot the corresponding trajectories of E_j ($j = 1, 2, 3, 4$) in Fig. 3(b). Here we show that for one complete cycle around the singularity in the parameter plane, the coupled eigenvalues E_1 and E_2 are permuted by exchanging their identities and make a complete loop in the complex-eigenvalue plane, whereas the unaffected states E_3 and E_4 remain to make individual loops. The corresponding insets in Fig. 3(b) show close-ups of the trajectories of E_3 and E_4 . Such unconventional state dynamics in the complex-eigenvalue plane proves that the identified second-order singularity between E_1 and E_2 behaves as an EP2 [5,14,15,22–26]. In Fig. 3(b) we show the state dynamics in the complex-eigenvalue plane concerning the parameter λ_R ; however, similar state dynamics can also be observed with respect to the parameters λ_I and δ .

After exploring the EP2 in the proposed system, we look into the parametric region where $E_1, E_2,$ and E_3 (except E_4)

are mutually coupled [as shown in Fig. 1(b)]. To enclose this region, we perform an encirclement process by choosing the characteristic parameters of Eq. (8) as $a_0 = 0.55, b_0 = -0.028, r_1 = 0.15,$ and $r_2 = 0.55$. These parameters are chosen in such a way that the resulting parameter space, shown in Fig. 4(a), encloses the third-order singularity in addition to the EP2 (between E_1 and E_2 only, as described in Fig. 3). Thus, we can examine the effects of the third-order singularity even in the presence of a different lower-order singularity. Now following a quasistatic encirclement process along the closed loop shown in Fig. 4(a), we plot the dynamics of E_j ($j = 1, 2, 3, 4$) in Fig. 4(b) concerning the parameter λ_R (however, instead of λ_R , we can also choose λ_I or δ). Here three coupled eigenvalues $E_1, E_2,$ and E_3 flip successively by exchanging their identities adiabatically in the complex-eigenvalue plane for one complete loop in the parametric plane. However, the noninteracting state E_4 is not affected by the dynamics of the other three states and keeps its self-identity by making

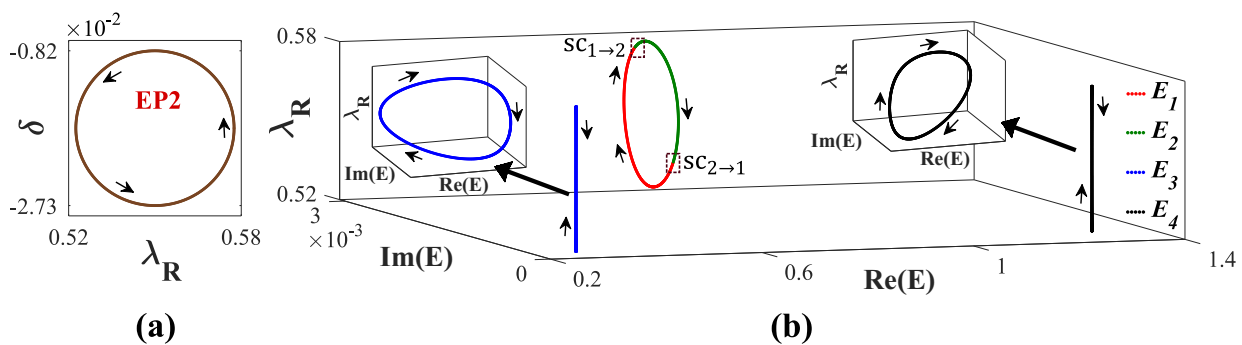


FIG. 3. State-flipping between a pair of coupled states. (a) Encircling an EP2 in the (λ_R, δ) plane. (b) Corresponding dynamics of E_j ($j = 1, 2, 3, 4$) in the complex E plane with respect to λ_R showing the flipping between the coupled E_1 and E_2 . The insets show close-ups of the trajectories of E_3 and E_4 for proper visualization. The state-conversion phenomena in the E plane are shown clearly inside the brown boxes, where the corresponding $SC_{i \rightarrow j}$ (with $\{i, j\} \in \{1, 2, 3, 4\}, i \neq j$) refers to the conversion from the i th state to the j th state. Arrows in both (a) and (b) indicate the direction of progression.

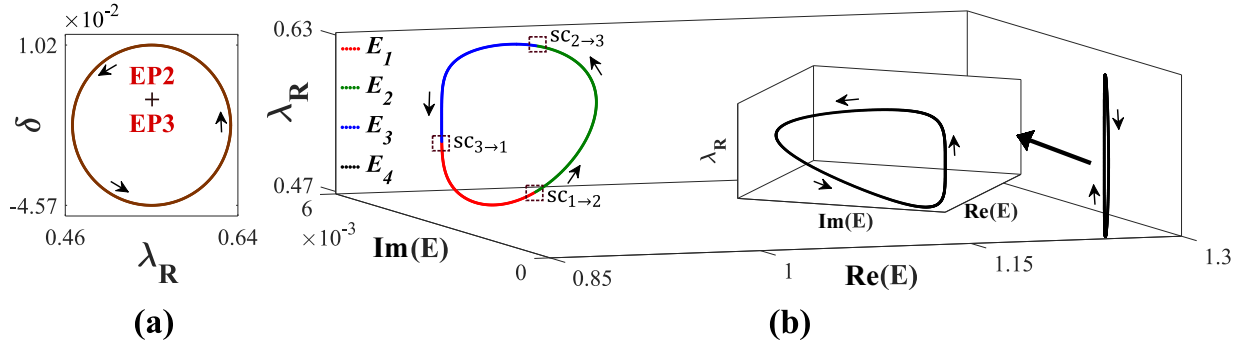


FIG. 4. Successive state flipping between three coupled states. (a) Parametric variation enclosing an EP2 and an EP3 in the (λ_R, δ) plane. (b) Corresponding dynamics of E_j ($j = 1, 2, 3, 4$) in the complex E plane with respect to λ_R showing the successive flipping between the coupled E_1, E_2 , and E_3 . The inset shows a close-up of the trajectory of E_4 for proper visualization. Arrows in both (a) and (b) indicate the direction of progression.

an individual loop. The magnified view of the trajectory of E_4 is shown in the inset. Such state dynamics in the complex-eigenvalue plane, as shown in Fig. 4(b), following the parameter space, as shown in Fig. 4(a), clearly justifies that the enclosed third-order singularity between E_1, E_2 , and E_3 behaves as an EP3 [10,11,29]. Here the exotic effect of the identified EP3 on the state dynamics is robust even in the presence of an EP2 inside the parametric loop. If we choose a similar parameter space that only encircles the approximate position of the EP3, even then one should observe similar state dynamics in the complex-eigenvalue plane.

Successfully verifying the topological properties of an EP2 and an EP3, we then study the dynamics of the proposed four-level Hamiltonian \mathcal{H} [Eq. (1)]. We encircle the approximate position of the embedded fourth-order singularity where

all four supported states E_j ($j = 1, 2, 3, 4$) are analytically connected. Accordingly, we choose the characteristics parameters of Eq. (8) as $a_0 = 0.55, b_0 = -0.019, r_1 = 0.5$, and $r_2 = 3.4$. Such a set of parameters also gives the opportunity to study the immutable behavior of the fourth-order singularity even in the presence of the EP2 and EP3 encountered. The chosen parametric contour is shown in Fig. 5(a). In Fig. 5(b) we study the corresponding dynamics of E_j ($j = 1, 2, 3, 4$) following a quasistatic parametric variation along the loop described in Fig. 5(a). As shown in Fig. 5(b), following one complete parametric cycle, all the coupled eigenvalues successively exchange their identities and make a complete loop in the complex-eigenvalue plane. Here the state dynamics are shown with respect to the parameter λ_R . In Fig. 5(c) we show similar successive state-flipping phenomena concerning

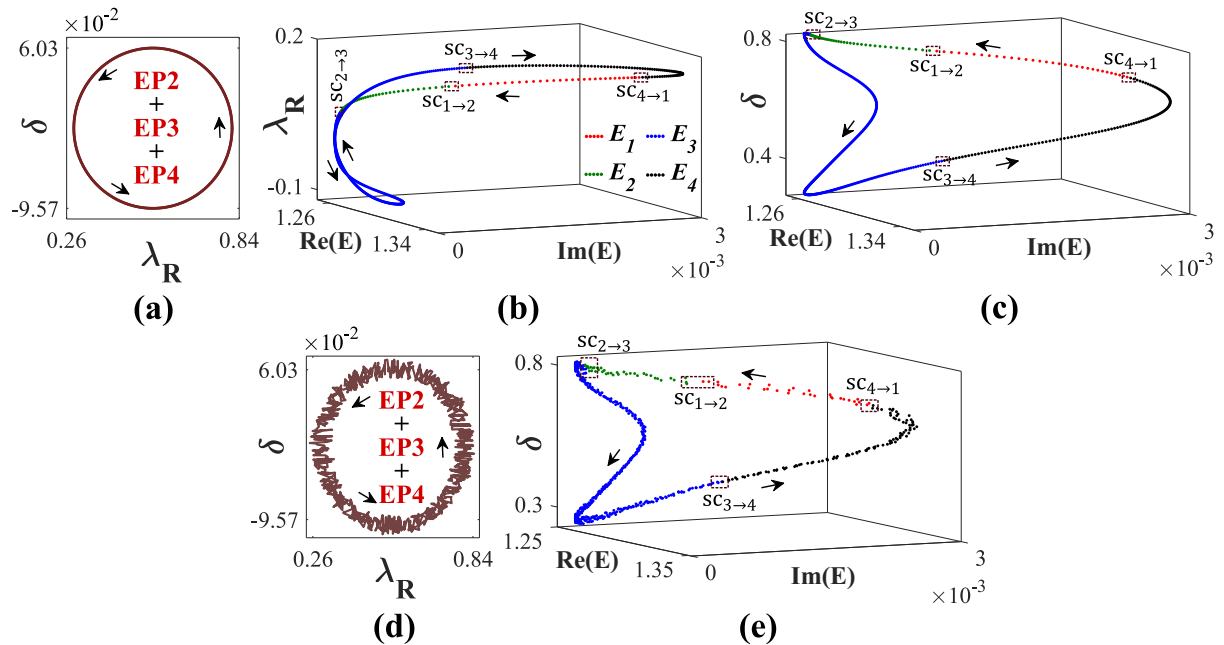


FIG. 5. Successive state flipping between four coupled states. (a) Parametric encirclement around an EP2, an EP3, and an EP4 in the (λ_R, δ) plane. The corresponding dynamics of E_j ($j = 1, 2, 3, 4$) in the complex E plane with respect to (b) λ_R and (c) δ show the successive flipping between all the coupled states. (d) Parametric encirclement similar to that shown in (a) with additional fluctuation. (e) Corresponding dynamics of E_j ($j = 1, 2, 3, 4$) in the complex E plane with respect to δ . Arrows in (a)–(e) indicate the direction of progression.

the parameter δ , for the exact same parametric loop. Such state dynamics confirms the exceptional nature of the embedded fourth-order singularity as an EP4. Thus we have successfully explored an exclusive state exchange among the four coupled states around an EP4. We also observe that there is no effect of the EP2 and EP3 on the state dynamics if an EP4 is properly enclosed in the system parameter space. During implementation of the proposed scheme in any realistic system, some unwanted tolerance may appear during the parametric encirclement process. To take into account such fabrication tolerances, we add some random fluctuations (up to $\sim 10\%$) on variation of the parameters following the same parametric loop as shown in Fig. 5(a). The modified parametric loop and corresponding state dynamics are shown in Figs. 5(d) and 5(e), respectively. Investigating the state dynamics as shown in Fig. 5(e), we can conclude that the successive state-flipping phenomenon around an EP4 is robust even in the presence of the parametric fluctuation. However, this is robust until the amount of fluctuation does not affect the approximate location of the EP4.

Note that, to facilitate matter, we do not consider the explicit time dependence of the parametric variation for the proposed Hamiltonian \mathcal{H} [given by Eq. (1)]. Thus, within this framework, the dynamical EP encirclement process and corresponding nonadiabatic chiral state-transfer phenomenon cannot be realized. In this work we straightforwardly investigate the dynamics of four complex eigenvalues in the vicinity of an EP4 and investigate corresponding topological properties. Based on the proposed model, any prototypal device

having the parameters with an explicit dependence on time or analogous length, e.g., any guided wave geometry having at least four channels or cores, may exhibit nonadiabatic modal propagation, which is still under investigation.

V. ANALYTIC PICTURE OF AN EP4

Here we describe the analytic structure of the eigenvalues and the corresponding eigenfunctions near an EP4 [6]. To describe the peculiar nature of the fourfold coalescence in the Hamiltonian \mathcal{H} ($=H_0 + \lambda H_p$) [given by Eq. (1)], we consider a particular point λ_c , where four levels are analytically connected, and a critical eigenvalue E_c at $\lambda = \lambda_c$. To consider such four-level coalescence through a fourth-root branch point, the set of equations

$$\frac{d^k}{dE^k} \det |\mathcal{H}(\lambda) - EI| = 0, \quad k = 0, 1, 2, 3, \quad (9)$$

must be satisfied simultaneously. Now the general set of eigenvalues E_j ($j = 1, 2, 3, 4$) can be written in terms of λ_c and E_c as

$$E_j(\lambda) = E_c + \sum_{l=1}^{\infty} a_l (\sqrt[4]{\lambda - \lambda_c})^l \quad \text{with } j = 1, 2, 3, 4. \quad (10)$$

Here a_l represent some real constants; $j = 1, 2, 3, 4$ represent the levels that are defined by the quantity $(\sqrt[4]{\lambda - \lambda_c})$ on the first, second, third, and fourth Riemann sheets in the λ plane. After expanding, Eq. (10) can be written more explicitly as

$$E_j(\lambda) = E_c + \sum_{l=1}^{\infty} a_l \left[\sqrt[4]{|\lambda - \lambda_c|} \exp\left(\frac{i \arg(\lambda - \lambda_c) + 2i\pi(j-1)}{4}\right) \right]^l. \quad (11)$$

Considering a critical eigenfunction at the EP4 as $|\psi_{\text{EP4}}\rangle$, the structure of the corresponding eigenfunctions can be written as

$$|\psi_j(\lambda)\rangle = |\psi_{\text{EP4}}\rangle + \sum_{l=1}^{\infty} (\sqrt[4]{\lambda - \lambda_c})^l |\phi_k\rangle. \quad (12)$$

Specifically considering four Riemann sheets for $j = 1, 2, 3, 4$, these eigenfunctions can be written more explicitly as

$$|\psi_j(\lambda)\rangle = |\psi_{\text{EP4}}\rangle + \sum_{l=1}^{\infty} (\sqrt[4]{\lambda - \lambda_c})^l |\phi_k^j\rangle, \quad (13)$$

with $|\phi_k^j\rangle = \exp[i \arg(\lambda - \lambda_c)/4 + 2i\pi(j-1)/4] |\phi_k\rangle$. Now all the possible pairs of eigenfunctions given by Eq. (13) form the usual biorthogonal complete system for all $\lambda \neq \lambda_c$ as

$$\langle \tilde{\psi}_i(\lambda) | \psi_j(\lambda) \rangle = N_j(\lambda) \delta_{i,j}, \quad (14a)$$

$$\sum_j \frac{|\psi_j(\lambda)\rangle \langle \tilde{\psi}_j(\lambda)|}{\langle \tilde{\psi}_j(\lambda) | \psi_j(\lambda) \rangle} = I. \quad (14b)$$

As for complex λ the corresponding Hamiltonian is not self-adjoint, in Eq. (14) $\tilde{\psi}$ and ψ have been used to differentiate left and right eigenvectors. Now the scalar product given by

Eq. (14a) vanishes as

$$N_j(\lambda) \sim \zeta (\sqrt[4]{\lambda - \lambda_c})^3 \quad \text{for } \lambda \rightarrow \lambda_c, \quad (15)$$

and then replacing one of the eigenfunctions of this product [given by Eq. (14a)] with the critical eigenfunction $|\psi_{\text{EP4}}\rangle$, we can write

$$\langle \tilde{\psi}_i(\lambda) | \psi_{\text{EP4}} \rangle \sim \vartheta (\sqrt[4]{\lambda - \lambda_c})^3 \quad \text{for } \lambda \rightarrow \lambda_c, \quad (16)$$

with some constants ζ and ϑ . Thus, once we consider $\lambda \rightarrow \lambda_c$,

$$\langle \tilde{\psi}_{\text{EP4}} | \psi_{\text{EP4}} \rangle = 0 \quad (17)$$

even if $i \neq j$, which means the coalescence of the eigenvectors. In addition, if $|\phi_1\rangle$ is associated with the first power of $(\sqrt[4]{\lambda - \lambda_c})$ in Eq. (12), then $\langle \tilde{\psi}_{\text{EP4}} | \phi_1 \rangle$ should also vanish.

Around the EP4, we can write the $|\psi_{\text{EP4}}\rangle$ as the linear combination of the coupled eigenvectors $|\chi_j(\lambda)\rangle$ with some constants c_j like

$$|\psi_{\text{EP4}}\rangle = \sum_{j=1}^4 c_j(\lambda) |\chi_j(\lambda)\rangle, \quad (18a)$$

with

$$|\chi_j(\lambda)\rangle = \frac{|\psi_j(\lambda)\rangle}{\sqrt{\langle \tilde{\psi}_j(\lambda) | \psi_j(\lambda) \rangle}}. \quad (18b)$$

The solutions of Eq. (18a) while $\lambda \rightarrow \lambda_c$ would yield the basic structure of the general eigenfunction with the corresponding phase relations based upon the fourth roots of unity. The possible combinations of c_j are given by

$$\begin{pmatrix} c_1(\lambda) \\ c_2(\lambda) \\ c_3(\lambda) \\ c_4(\lambda) \end{pmatrix} \sim \kappa_1 \sqrt[4]{|\lambda - \lambda_c|} \begin{pmatrix} 1 \\ e^{+i\pi/2} \\ e^{i\pi} \\ e^{-i\pi/2} \end{pmatrix}, \quad (19a)$$

$$\begin{pmatrix} c_1(\lambda) \\ c_2(\lambda) \\ c_3(\lambda) \\ c_4(\lambda) \end{pmatrix} \sim \kappa_2 \sqrt[4]{|\lambda - \lambda_c|} \begin{pmatrix} e^{-i\pi/2} \\ e^{+i\pi/2} \\ 1 \\ e^{i\pi} \end{pmatrix}, \quad (19b)$$

$$\begin{pmatrix} c_1(\lambda) \\ c_2(\lambda) \\ c_3(\lambda) \\ c_4(\lambda) \end{pmatrix} \sim \kappa_3 \sqrt[4]{|\lambda - \lambda_c|} \begin{pmatrix} e^{+i\pi/2} \\ e^{i\pi} \\ 1 \\ e^{-i\pi/2} \end{pmatrix}, \quad (19c)$$

$$\begin{pmatrix} c_1(\lambda) \\ c_2(\lambda) \\ c_3(\lambda) \\ c_4(\lambda) \end{pmatrix} \sim \kappa_4 \sqrt[4]{|\lambda - \lambda_c|} \begin{pmatrix} e^{+i\pi/2} \\ e^{-i\pi/2} \\ e^{i\pi} \\ 1 \end{pmatrix}. \quad (19d)$$

Here κ_j ($j = 1, 2, 3, 4$) are some complex constants. We also obtain that the divergence of $|\chi_j(\lambda)\rangle$ will lead to a finite value of $|\psi_{EP4}\rangle$. Thus, from Eq. (18), we further conclude that

$$\sum_{j=1}^4 c_j(\lambda) = 0, \quad (20)$$

since $\langle \tilde{\psi}_{EP4} | \psi_{EP4} \rangle = 0$. Mathematically, Eq. (20), which resembles the chirality condition around the EP2, also leads to the chiral nature of coupled states around an EP4.

VI. FORMULATION OF A REGION TO HOST MULTIPLE EP4S: EXCEPTIONAL REGION

In this section we study the specific relations between the perturbation parameters (which are connected by a specific parameter δ) and the independent coupling control parameter λ to formulate a specific parametric region in which the fourth-order coupling can occur multiple times. This specific parametric region is referred to as the EP4 region, i.e., this region can host multiple EP4s.

To describe such a region we make some special settings in our proposed Hamiltonian \mathcal{H} given in Eq. (1). Initially, to facilitate the situation, we consider $\omega_s = 1$ and rewrite Eq. (1) as

$$\mathcal{H}|_{\omega_s=1} = \begin{pmatrix} \tilde{\varepsilon}_1 & \omega_p \lambda & 0 & \omega_q \lambda \\ \omega_p \lambda & \tilde{\varepsilon}_2 & \omega_r \lambda & 0 \\ 0 & \omega_r \lambda & \tilde{\varepsilon}_3 & 0 \\ \omega_q \lambda & 0 & 0 & \tilde{\varepsilon}_4 \end{pmatrix} + \lambda \begin{pmatrix} 0 & 0 & 0 & 0 \\ 0 & 0 & 0 & 0 \\ 0 & 0 & 0 & 1 \\ 0 & 0 & 1 & 0 \end{pmatrix}. \quad (21)$$

Such special consideration has been made to explore the relation of ω_p to ω_q and ω_r over the independent variation of λ . In this case Eq. (2) can be rewritten as

$$E^4 + p_1 E^3 + p'_2 E^2 + p'_3 E + p'_4 = 0, \quad (22)$$

where p_1 is given by Eq. (3a) and p'_2 , p'_3 , and p'_4 are from Eqs. (3b), (3c), and (3d), respectively, considering the special setting $\omega_s = 1$. Now considering the fourfold coalescence at an EP4, we rigorously assume a critical eigenvalue, which is the mean of all passive elements, at the coalescing point as

$$E_c = \frac{1}{4}(\tilde{\varepsilon}_1 + \tilde{\varepsilon}_2 + \tilde{\varepsilon}_3 + \tilde{\varepsilon}_4), \quad (23)$$

which must satisfy Eq. (22). Again, extracting the terms containing ω_p from p'_2 , p'_3 , and p'_4 as

$$p'_2 = p''_2 - \lambda^2 \omega_p^2, \quad (24a)$$

$$p'_3 = p''_3 + \lambda^2 (\tilde{\varepsilon}_3 + \tilde{\varepsilon}_4) \omega_p^2, \quad (24b)$$

$$p'_4 = p''_4 - \lambda^2 \tilde{\varepsilon}_3 \tilde{\varepsilon}_4 \omega_p^2 - \lambda^4 (\omega_p^2 + 2\omega_p \omega_q \omega_r), \quad (24c)$$

we can rewrite Eq. (22) as

$$\mu_1 \omega_p^2 + \mu_2 \omega_p + \mu_3 = 0, \quad (25)$$

with

$$\mu_1 = \lambda^2 (\tilde{\varepsilon}_3 + \tilde{\varepsilon}_4 - \tilde{\varepsilon}_3 \tilde{\varepsilon}_4 - \lambda^2 - E_c^2), \quad (26a)$$

$$\mu_2 = -2\lambda^4 \omega_q \omega_r, \quad (26b)$$

$$\mu_3 = E_c^4 + p_1 E_c^3 + p'_2 E_c^2 + p'_3 E_c + p'_4. \quad (26c)$$

Here $\{p''_2, p''_3, p''_4\}$ represent the parameters $\{p'_2, p'_3, p'_4\}$ after extraction of the ω_p terms. If we write ω_r in terms of ω_q using the relation $\omega_r = 0.95 - (\omega_q + 0.1)/2$ [from Eqs. (7a) and (7b)], then Eq. (25) becomes a pure quadratic equation of ω_p having two different roots, say, ω_p^+ and ω_p^- .

Now we consider a different special setting in Eq. (1) as $\omega_p = 1$ to explore the relation of ω_s to ω_q and ω_r over the independent variation of λ . We rewrite Eq. (1) as

$$\mathcal{H}|_{\omega_p=1} = \begin{pmatrix} \tilde{\varepsilon}_1 & 0 & 0 & \omega_q \lambda \\ 0 & \tilde{\varepsilon}_2 & \omega_r \lambda & 0 \\ 0 & \omega_r \lambda & \tilde{\varepsilon}_3 & \omega_s \lambda \\ \omega_q \lambda & 0 & \omega_s \lambda & \tilde{\varepsilon}_4 \end{pmatrix} + \lambda \begin{pmatrix} 0 & 1 & 0 & 0 \\ 1 & 0 & 0 & 0 \\ 0 & 0 & 0 & 0 \\ 0 & 0 & 0 & 0 \end{pmatrix}. \quad (27)$$

Also considering the critical eigenvalue E_c [given by Eq. (23)] and the relation between ω_r and ω_q as $\omega_r = 0.95 - (\omega_q + 0.1)/2$ [from Eqs. (7a) and (7b)], we can derive a pure quadratic equation of ω_s having the form

$$v_1 \omega_s^2 + v_2 \omega_s + v_3 = 0. \quad (28)$$

Expressions for the terms v_1 , v_2 , and v_3 can be obtained in a similar way, which is described for the previous special setting. Equation (28) has two different roots, ω_s^+ and ω_s^- .

Now we plot the roots $\{\omega_p^+, \omega_p^-\}$ [from Eq. (25), represented by dotted blue and red curves, respectively] and $\{\omega_s^+, \omega_s^-\}$ [from Eq. (28), represented by dotted magenta and black curves, respectively] in Fig. 6(a) for a continuous variation of λ_R within $[-2, 2]$ (with simultaneous variation of λ_I maintaining the ratio $\lambda_I/\lambda_R = -10^{-3}$), taking different values of ω_q . Here we investigate the intersecting region

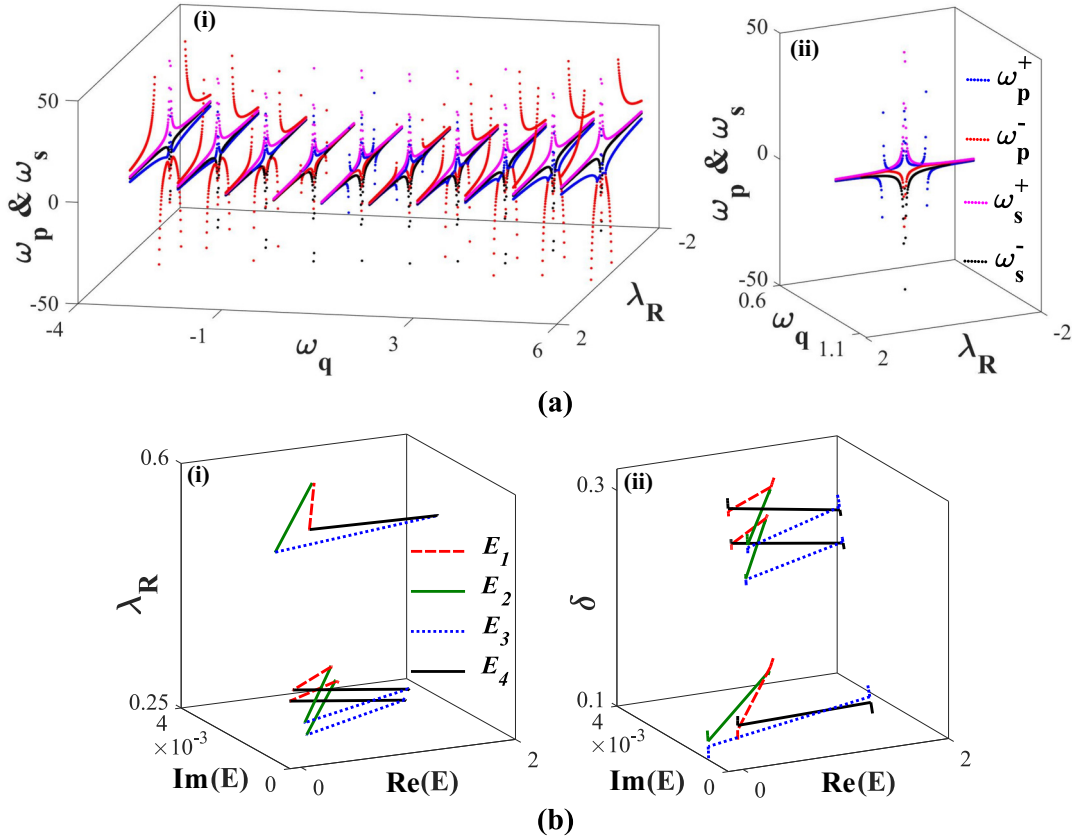


FIG. 6. The EP4 region and the existence of multiple EP4s. (a) (a i) Variation of perturbation parameters with respect to λ_R forming a 3D region that hosts multiple EP4s. (a ii) Specific cross section of the region shown in (a i). (b) Existence of multiple EP4s governing the interactions between all the coupled states with respect to (b i) λ_R and (b ii) δ inside the region shown in (a i).

between the trajectories of these four roots. As can be seen in Fig. 6(a i), we observe that for $\omega_q = -3.14$, there is no blank area under the intersections. Then, for an increasing ω_q , the area under the intersections increases up to a specific value of $\omega_q = 0.86$ and then decreases again even we increase ω_q further. For $\omega_q = 5.86$, again there is no blank area under the intersections. If we consider the overall range of ω_q from -3.14 to 5.86 , then we can realize a closed 3D space in Fig. 6(a i). A particular cross section of this closed 3D space, where the area under the intersections becomes maximum, i.e., for $\omega_q = 0.86$, is shown in Fig. 6(a ii).

We refer to this closed 3D space as the EP4 region because within this region the proper coupling between the perturbation parameters ω_p , ω_q , ω_r , and ω_s through δ for a continuous variation of λ will happen to control the fourth-order interactions between four states of the proposed Hamiltonian \mathcal{H} [given by Eq. (1)]. Thus, in Fig. 6(a i), we show the relation between ω_p and ω_s with ω_q and ω_r for a wide range of λ where ω_r has been expressed in terms of ω_q . If we express ω_q in terms of ω_r then we can also get a region similar to that shown in Fig. 6(a i), but in this case the ω_q axis will be replaced by the ω_r axis. Note that, in this calculation, we consider two special settings by choosing a specific pair $\{\omega_p, \omega_s\}$ from four perturbation parameters. In a very similar way we can choose a different pair from the possible combinations to formulate such an EP4 region. Winding around this parametric region shown in Fig. 6(a i), we encounter three different situations for

the proposed Hamiltonian \mathcal{H} where four states are mutually interacting around three different EP4s. In Fig. 6(b i) we show three such fourth-order interactions within the EP4 region with respect to λ_R . For proper validation, we show the same interactions between four coupled states with respect to δ in Fig. 6(b ii).

VII. CONCLUSION

In summary, we have reported the existence of a fourth-order exceptional point (EP4) by considering a four-level non-Hermitian Hamiltonian. Within the proposed framework, a passive system, hosting four decaying states, is subjected to a parameter-dependent perturbation. We have chosen a complex (λ) and a real (δ) control parameter in such a way that the system can host different orders of interaction phenomena between the supported states in the vicinity of different orders of singularities. We have shown the simultaneous existence of an EP2, an EP3, and an EP4 within a certain parametric range. Verifying the state-exchange phenomenon between two and three coupled states around an EP2 and an EP3, respectively, we have established a successive state-conversion phenomenon between four coupled states following a parametric variation around an EP4. Introducing random fluctuation in the parametric variation around an EP4, the immutability of this successive state-conversion phenomenon has been shown. We have also established that the topological properties of

an EP of a specific order are robust even in the presence of other EPs of lower order inside the parametric loop. To correlate the multiple locations of EP4s in a system, we have formulated an EP4 region by the interplay between the specific relationship of perturbation parameters and the coupling control parameters. The chiral behavior of the state-exchange phenomenon around the EP4 has also been established. The systems realized with such a scheme may provide a fertile foundation to improve the quality of a wide range of EP-aided state-of-the-art applications such as all-optical mode conversions and optical sensing with enhanced sensitivity. Owing to

unconventional, richer physical aspects, an EP4 could provide an alternative light manipulation tool in integrated circuits.

ACKNOWLEDGMENTS

S.B. acknowledges support from Ministry of Human Resource Development, India. A.L. and S.G. acknowledge financial support from the Science and Engineering Research Board, Ministry of Science and Technology, India under Early Career Research Scheme; Grant No. ECR/2017/000491.

-
- [1] N. Moiseyev, *Non-Hermitian Quantum Mechanics* (Cambridge University Press, New York, 2011).
- [2] T. Kato, *Perturbation Theory of Linear Operators* (Springer, Berlin, 1995).
- [3] W. D. Heiss, The physics of exceptional points, *J. Phys. A: Math. Theor.* **45**, 444016 (2012).
- [4] W. D. Heiss and A. L. Sannino, Avoided level crossing and exceptional points, *J. Phys. A: Math. Gen.* **23**, 1167 (1990).
- [5] W. D. Heiss, Repulsion of resonance states and exceptional points, *Phys. Rev. E* **61**, 929 (2000).
- [6] W. D. Heiss, Chirality of wavefunctions for three coalescing levels, *J. Phys. A: Math. Theor.* **41**, 244010 (2008).
- [7] G. Demange and E.-M. Graefe, Signatures of three coalescing eigenfunctions, *J. Phys. A: Math. Theor.* **45**, 025303 (2012).
- [8] W. D. Heiss and G. Wunner, A model of three coupled wave guides and third order exceptional points, *J. Phys. A: Math. Theor.* **49**, 495303 (2016).
- [9] J.-W. Ryu, S.-Y. Lee, and S. W. Kim, Analysis of multiple exceptional points related to three interacting eigenmodes in a non-Hermitian Hamiltonian, *Phys. Rev. A* **85**, 042101 (2016).
- [10] S. Bhattacharjee, A. Laha, and S. Ghosh, Encounter of higher order exceptional singularities and towards cascaded state conversion, *Phys. Scr.* **94**, 085202 (2019).
- [11] S. Bhattacharjee, A. Laha, and S. Ghosh, Topological dynamics of an adiabatically varying Hamiltonian around third order exceptional points, *Phys. Scr.* **94**, 105509 (2019).
- [12] L. Pan, S. Chen, and X. Cui, High-order exceptional points in ultracold Bose gases, *Phys. Rev. A* **99**, 011601(R) (2019).
- [13] Y.-X. Xiao, Z.-Q. Zhang, Z. H. Hang, and C. T. Chan, Anisotropic exceptional points of arbitrary order, *Phys. Rev. B* **99**, 241403(R) (2019).
- [14] H. Cartarius, J. Main, and G. Wunner, Exceptional Points in Atomic Spectra, *Phys. Rev. Lett.* **99**, 173003 (2007).
- [15] H. Menke, M. Klett, H. Cartarius, J. Main, and G. Wunner, State flip at exceptional points in atomic spectra, *Phys. Rev. A* **93**, 013401 (2016).
- [16] R. Lefebvre, O. Atabek, M. Šindelka, and N. Moiseyev, Resonance Coalescence in Molecular Photodissociation, *Phys. Rev. Lett.* **103**, 123003 (2009).
- [17] B. Dietz, H. L. Harney, O. N. Kirillov, M. Miski-Oglu, A. Richter, and F. Schäfer, Exceptional Points in a Microwave Billiard with Time-Reversal Invariance Violation, *Phys. Rev. Lett.* **106**, 150403 (2011).
- [18] R. Gutöhrlein, J. Main, H. Cartarius, and G. Wunner, Bifurcations and exceptional points in dipolar Bose-Einstein condensates, *J. Phys. A: Math. Theor.* **46**, 305001 (2013).
- [19] E. M. Graefe, U. Günther, H. J. Korsch, and A. E. Niederle, A non-Hermitian \mathcal{PT} -symmetric Bose-Hubbard model: Eigenvalue rings from unfolding higher-order exceptional points, *J. Phys. A: Math. Theor.* **41**, 255206 (2008).
- [20] H. Hodaei, A. U. Hassan, W. E. Haynga, A. M. Miri, D. N. Christodoulides, and M. Khajavikhan, Dark-state lasers: Mode management using exceptional points, *Opt. Lett.* **41**, 3049 (2016).
- [21] Z. J. Wong, Y.-L. Xu, J. Kim, K. O'Brien, Y. Wang, L. Feng, and X. Zhang, Lasing and anti-lasing in a single cavity, *Nat. Photon.* **10**, 796 (2016).
- [22] A. Laha and S. Ghosh, Connected hidden singularities and toward successive state flipping in degenerate optical microcavities, *J. Opt. Soc. Am. B* **34**, 238 (2017).
- [23] A. Laha, A. Biswas, and S. Ghosh, Next-nearest-neighbor resonance coupling and exceptional singularities in degenerate optical microcavities, *J. Opt. Soc. Am. B* **34**, 2050 (2017).
- [24] A. Laha, A. Biswas, and S. Ghosh, Minimally asymmetric state conversion around exceptional singularities in a specialty optical microcavity, *J. Opt.* **21**, 025201 (2019).
- [25] S. Ghosh and Y. D. Chong, Exceptional points and asymmetric mode conversion in quasi-guided dual-mode optical waveguides, *Sci. Rep.* **6**, 19837 (2016).
- [26] A. Laha, A. Biswas, and S. Ghosh, Nonadiabatic Modal Dynamics Around Exceptional Points in an All-Lossy Dual-Mode Optical Waveguide: Toward Chirality-Driven Asymmetric Mode Conversion, *Phys. Rev. Appl.* **10**, 054008 (2018).
- [27] X. L. Zhang, S. Wang, B. Hou, and C. T. Chan, Dynamically Encircling Exceptional Points: *In Situ* Control of Encircling Loops and the Role of the Starting Point, *Phys. Rev. X* **8**, 021066 (2018).
- [28] X. L. Zhang and C. T. Chan, Dynamically encircling exceptional points in a three-mode waveguide system, *Commun. Phys.* **2**, 63 (2019).
- [29] J. Schnabel, H. Cartarius, J. Main, G. Wunner, and W. D. Heiss, \mathcal{PT} -symmetric waveguide system with evidence of a third-order exceptional point, *Phys. Rev. A* **95**, 053868 (2017).
- [30] K. Ding, Z. Q. Zhang, and C. T. Chan, Coalescence of exceptional points and phase diagrams for one-dimensional \mathcal{PT} -symmetric photonic crystals, *Phys. Rev. B* **92**, 235310 (2015).
- [31] D. A. Bykov and L. L. Doskolovich, Cross-polarization mode coupling and exceptional points in photonic crystal slabs, *Phys. Rev. A* **97**, 013846 (2018).
- [32] X. Yin and X. Zhang, Unidirectional light propagation at exceptional points, *Nat. Mater.* **12**, 175 (2013).

- [33] H. Xu, D. Mason, L. Jiang, and J. G. E. Harris, Topological energy transfer in an optomechanical system with exceptional points, *Nature (London)* **537**, 80 (2016).
- [34] W. D. Heiss and G. Wunner, Resonance scattering at third-order exceptional points, *J. Phys. A: Math. Theor.* **48**, 345203 (2015),
- [35] B. Midya and V. V. Konotop, Waveguides with Absorbing Boundaries: Nonlinearity Controlled by an Exceptional Point and Solitons, *Phys. Rev. Lett.* **119**, 033905 (2017).
- [36] J. Wiersig, Enhancing the Sensitivity of Frequency and Energy Splitting Detection by Using Exceptional Points: Application to Microcavity Sensors for Single-Particle Detection, *Phys. Rev. Lett.* **112**, 203901 (2014).
- [37] J. Wiersig, Sensors operating at exceptional points: General theory, *Phys. Rev. A* **93**, 033809 (2016).
- [38] H. Hodaei, A. U. Hassan, S. Wittek, H. Garcia-Gracia, R. El-Ganainy, D. N. Christodoulides, and M. Khajavikhan, Enhanced sensitivity at higher-order exceptional points, *Nature (London)* **548**, 187 (2017).
- [39] W. Chen, Ş. K. Özdemir, G. Zhao, J. Wiersig, and L. Yang, Exceptional points enhance sensing in an optical microcavity, *Nature (London)* **548**, 192 (2017).
- [40] R. Thomas, H. Li, F. M. Ellis, and T. Kottos, Giant nonreciprocity near exceptional-point degeneracies, *Phys. Rev. A* **94**, 043829 (2016).
- [41] Y. Choi, C. Hahn, J. W. Yoon, S. H. Song, and P. Berini, Extremely broadband, on-chip optical nonreciprocity enabled by mimicking nonlinear anti-adiabatic quantum jumps near exceptional points, *Nat. Commun.* **8**, 14154 (2017).
- [42] T. Goldzak, A. A. Mailybaev, and N. Moiseyev, Light Stops at Exceptional Points, *Phys. Rev. Lett.* **120**, 013901 (2018).
- [43] H. Jing, S. K. Özdemir, H. Lü, and F. Nori, High-order exceptional points in optomechanics, *Sci. Rep.* **7**, 3386 (2017).
- [44] Y.-P. Gao, C. Cao, T.-J. Wang, Y. Zhang, and C. Wang, Cavity-mediated coupling of phonons and magnons, *Phys. Rev. A* **96**, 023826 (2017).
- [45] H. Lü, S. K. Özdemir, L.-M. Kuang, F. Nori, and H. Jing, Exceptional Points in Random-Defect Phonon Lasers, *Phys. Rev. Appl.* **8**, 044020 (2017).
- [46] R. El-Ganainy, K. G. Makris, M. Khajavikhan, Z. H. Musslimani, S. Rotter, and D. N. Christodoulides, Non-Hermitian physics and PT symmetry, *Nat. Phys.* **14**, 11 (2018).
- [47] M. A. Miri and A. Alù, Exceptional points in optics and photonics, *Science* **363**, 42 (2019).
- [48] C. Dembowski, H.-D. Gräf, H. L. Harney, A. Heine, W. D. Heiss, H. Rehfeld, and A. Richter, Experimental Observation of the Topological Structure of Exceptional Points, *Phys. Rev. Lett.* **86**, 787 (2001).
- [49] C. Dembowski, B. Dietz, H.-D. Gräf, H. L. Harney, A. Heine, W. D. Heiss, and A. Richter, Encircling an exceptional point, *Phys. Rev. E* **69**, 056216 (2004).
- [50] S.-Y. Lee, J.-W. Ryu, S. W. Kim, and Y. Chung, Geometric phase around multiple exceptional points, *Phys. Rev. A* **85**, 064103 (2012).
- [51] I. Gilyary, A. A. Mailybaev, and N. Moiseyev, Time-asymmetric quantum-state-exchange mechanism, *Phys. Rev. A* **88**, 010102(R) (2013).
- [52] C. B. Boyer and U. C. Merzbach, *A History of Mathematics*, 2nd ed. (Wiley, New York, 1991).